Optical Spectra of Push−Pull Chromophores in Solution: A Simple Model

Anna Painelli* and Francesca Terenziani

Dipartimento di Chimica GIAF, Università di Parma, I-43100 Parma, Italy

Received: April 26, 2000; In Final Form: September 14, 2000

We extend the self-consistent two-state model, already proposed to describe linear and nonlinear spectral properties of push−pull chromophores in solution, to describe vibrational spectra and to account for inhomogeneous broadening effects occurring in polar solvents. The model, not relying on perturbative expansions of the solute−solvent interaction, offers a simple and internally consistent description of electronic and vibrational spectra. Exotic and apparently unrelated phenomena, like the narrowing of time-resolved emission bands and the dispersion of resonant Raman frequencies with the excitation line find a natural explanation in the proposed approach.

Introduction

The so-called push−pull chromophores are molecules made up by electron donor (D) and acceptor (A) moieties connected by a π-conjugated bridge. The charge separated state (D^+A^-) is then easily accessible. These molecules are widely investigated in several, apparently unrelated fields. Push−pull chromophores are the molecules of choice for second-order NLO applications,[1,2] are typical solvation probes,[3,4] and are useful model systems for electron transfer.[5] All these applications exploit the presence of a low-lying excited-state characterized by a different electronic distribution from the ground state. Good solvation probes have an electronic absorption and/or emission band well-separated from the other transitions, with good intensity (i.e., a sizable transition dipole moment, μ_{CT}), and whose position strongly depends on the solvent polarity.[3] This last requirement is easily fulfilled if the mesomeric dipole moment, i.e., the difference between the excited and the ground state (gs) dipole moment, is large. A large mesomeric dipole moment implies a large charge redistribution on excitation, so that the absorption process basically models a photoinduced electron transfer,[5] whereas the emission process models a nonradiative electron transfer.[5] On the other hand, large transition and mesomeric dipole moments are a guarantee of large NLO responses.[6]

The interesting behavior of push−pull chromophores is dominated by the lowest excited state, and a simple two-state model has indeed all the ingredients needed to catch the essential physics governing these molecules. The relevant two-state model, the DA dimer, was proposed in the 50's to describe charge transfer (CT) complexes.[7] And in fact CT complexes too are actively investigated as model systems for electron transfer.[5,8] Their investigation as NLO chromophores is certainly worthwhile. When extended to include the interaction with the surrounding and/or the coupling with vibrations (Holstein coupling) the DA dimer model is the simplest model for the neutral−ionic phase transition as observed in CT organic salts with a mixed stack motif.[9] The peculiar behavior of the interacting model opens new perspectives in modeling electron transfer, and, for what concerns us here, demonstrates the large nonlinearity of the response of the DA dimer to the relevant interactions.[10,11]

* Corresponding author: Phone: +39-0521-905461. Fax: +39-0521-905556. E-mail: painelli@unipr.it.

The intrinsic nonlinearity of the DA dimer is responsible for the large amplification of static NLO responses as due to the coupling of electronic degrees of freedom to molecular vibrations[10] or, equivalently, to the orientational polarization of polar solvents.[11] The slow degrees of freedom can be dealt with in the adiabatic approximation, and the resulting model, the self-consistent DA dimer model, is amenable to an exact solution.[10,11] The most prominent advantage of exact results is that they can be used to check the reliability of approximation schemes: quite predictably we were able to prove that linear perturbative approaches to the interactions are inadequate to describe the highly nonlinear behavior of push−pull chromophores.[11,12] This has important consequences, since the sum-over-state approach to the vibrational contribution to NLO responses, as commonly adopted in quantum chemical calculations, being based on a linear perturbative treatment of the electron-vibration (e−ph) coupling, is in general inadequate, and must be substituted by finite-field methods.

In a recent paper,[12] based on exact results for the self-consistent DA dimer, we demonstrated that nonlinearity plays an important role also in linear absorption and emission spectra. The nonlinearity of the solute−solvent interaction stems out apparently from the nonlinearity of the Stokes shifts with the solvent polarity, from the dependence of the absorption and emission band-shapes on the solvent, and from the observation of nonspecular absorption and emission bands. The standard approaches to solvatochromism[4,13] allow for linear corrections of the solute energies as due to the interaction with the solvent, but postulate that the solute wave functions are independent of solvation. This rigid-solute, perturbative approach fails for most of push−pull chromophores in view of their large linear and nonlinear polarizabilities: the solute properties largely depend on the solvation medium.

This nonlinearity has disruptive effects on our standard understanding of spectral data, that is mainly based on perturbative arguments. An impressive example is offered by absorption and emission bands: in the standard picture, the vibronic structure underlying the two bands is the same, so that exactly the same info can be extracted from the analysis of either of them.[5] This is not true for push−pull chromophores: after absorption, these largely polarizable molecules readjust their charge distribution following the relaxation of slow degrees of

10.1021/jp0016075 CCC: $19.00 © 2000 American Chemical Society
Published on Web 11/02/2000

freedom. Absorption and emission processes then involve different states and are governed by different parameters: the Huang−Rhys factors relevant to the two processes are indeed different.[12] Extracting microscopic information from spectral results is therefore a complex task in push−pull chromophores and requires a careful analysis of a large set of data, properly accounting for the nonlinearity of the system. Since in a nonlinear picture microscopic parameters are not directly related to any single experimental feature, it is important to cross check the reliability of the model and the accuracy of the parameters by a careful study of as many spectral data as possible.[12,14]

In this paper we extend the analysis of spectral properties of push−pull chromophores in solution to vibrational spectra. The e−ph coupling affects vibrational properties of coupled modes, that appear in both infrared (IR) and Raman spectra.[11] Specifically the interaction with electronic degrees of freedom softens coupled vibrations, and affects their intensities in a way that strongly depends on the molecular charge distribution, and therefore on the solvation medium. This dependence is also the key to understand the large inhomogeneous broadening effects appearing in vibrational spectra of molecules dissolved in polar solvents.[15,16] A careful analysis of vibrational spectra gives important information on e−ph coupling strength, and, more generally, if complemented with the analysis of absorption and emission spectra, allows for the estimate of the microscopic parameters of the model. This analysis must properly account for the nonlinearity of the chromophore: in push−pull chromophores, resonant Raman (RR) and steady-state emission spectra are governed by different Huang−Rhys factors, for exactly the same reason why absorption and emission bands are nonspecular. This is an important observation pointing to the need for a careful reconsideration of the analysis carried over electronic and RR spectra of a few model systems for electron transfer.[5,17,18] Hopefully some of the apparent discrepancies in these data can be settled in the new picture.

In the next section we briefly review the self-consistent DA dimer model as the simplest model for a push−pull chromophore in solution, with special emphasis on its application to linear absorption and emission spectra in the visible region. In section III we apply the model to vibrational (IR and Raman) spectra. In section IV the analysis is extended to account for inhomogeneous broadening as observed in polar solvents. The implications of the proposed model on the interpretation of spectral data are discussed in the last section. In the companion paper (the following article) we apply our model to a specific chromophore, phenol blue. This is an interesting molecule, with large measured nonlinear responses.[19] For this molecule with a highly nonlinear behavior, the standard analysis of spectral data is bound to fail, and in fact its spectra are characterized by several anomalous features, the most prominent one being the large dispersion of RR frequencies with the excitation line.[16] We will demonstrate that the exotic spectral behavior of PB is naturally understood based on the simple model we present here, provided its nonlinearity is fully exploited.

Simple Model for Electronic Properties

The electronic structure of push−pull chromophores can be described based on two states, the fully neutral, $|DA\rangle$, and the charge-separated, $|D^+A^-\rangle$ states. These two states correspond to the neutral and zwitterionic resonance structures of the molecule, or, in the context of charge transfer (CT) complexes, to the fully neutral and ionic states, as introduced by Mulliken.[7] Following Mulliken, we neglect the small dipole moment of $|DA\rangle$ with respect to μ_0, the large dipole moment of $|D^+A^-\rangle$.

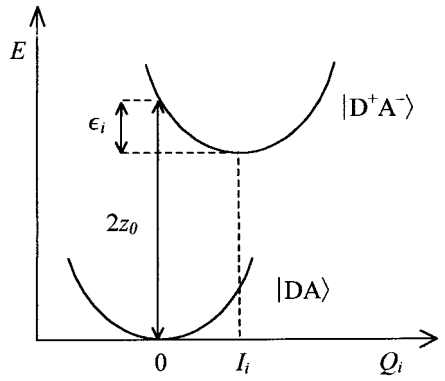

Figure 1. Potential energy surfaces relevant to the two basis states (see text).

We allow for the coupling of electrons to molecular vibrations, Q_i, by assigning the two basis states two harmonic potential energy surfaces (PES), with equal frequencies (ω_i), but displaced by I_i, as sketched in Figure 1. The corresponding Hamiltonian reads[10]

$$H = 2z_0\hat{\rho} - \sqrt{2}t\sigma_x + \sum_{i=1}^{N}\left\{\frac{1}{2}\omega_i^2 Q_i^2 - \sqrt{2\omega_i}g_i Q_i\hat{\rho}\right\} \quad (1)$$

where z_0 is half the energy difference between the two basis states, measured at $Q_i = 0$ (see Figure 1), and $\sqrt{2}t$ allows for the mixing of the two states. Unless when energy units are explicitly given, in the following we measure the energy in $\sqrt{2}t = 1$ units. Adopting the standard notation for Pauli spin operators ($\sigma_{x,y,z}$), the ionicity operator, $\hat{\rho} = (1 - \sigma_z)/2$, measures the polarity of the molecule, i.e., the weight of $|D^+A^-\rangle$. The summation in eq 1 runs on the N totally symmetric vibrations that couple to electrons. The first term in the summation accounts for the vibrational potential energy (consistently with the adiabatic approximation we neglect the vibrational kinetic energy). The second term models e−ph coupling, with $g_i = I_i\omega_i^{3/2}/\sqrt{2}$ representing the e−ph coupling constant, as usually defined in the Holstein model.[20] A useful measure of the strength of e−ph coupling is $\epsilon_i = g_i^2/\omega_i$, that corresponds to the energy gained by the system due to the relaxation of Q_i following the charge separation (cf. Figure 1). The total vibrational relaxation energy, $\epsilon_{sp} = \Sigma_i\epsilon_i$, corresponds to the small polaron binding energy of the Holstein model.[20]

The very last term in the above Hamiltonian introduces a linear dependence of z_0 on the Q_i's, and then accounts for different equilibrium geometries in the two basis states. Quadratic terms would also account for different force constants, and then for different curvatures for the two PES in Figure 1. The role of quadratic coupling in Holstein-like Hamiltonian has been extensively investigated in ref 21. In the analysis of vibrational spectra of CT salts, quadratic e−ph coupling is routinely introduced to properly define reference vibrational frequencies for states of intermediate ionicity.[21,22] For these systems reliable information on the parameters required to model quadratic coupling are easily extracted from vibrational spectra of isolated donor and acceptor molecules and of the corresponding ions (D^+ and A^-, respectively). This information is not available for push−pull chromophores so that introducing quadratic e−ph coupling is not difficult per se, but adds the Hamiltonian several freely adjustable parameters. Since the basic physics of the problem is described by the linear term,[22] we neglect quadratic e−ph coupling in our model, adopting the simplest relevant Hamiltonian.

The simplest model for the solute−solvent interaction is the reaction-field model.[13,23] Basically, a polar solute molecule polarizes the surrounding medium and therefore feels a reaction electric field F_R. In the plausible hypothesis that the solvent is an optically linear medium, and then responds linearly to an applied field, the reaction field is simply proportional to the dipole moment of the solute molecule. The reaction field has in general two components.[13,23] One component originates from the deformation of the electronic clouds of solvent molecules. This "electronic" component of the reaction field is characterized by a very fast response time: it is in fact related to the electronic polarizability of the solvent, with typical frequencies in the UV region, to be compared with typical frequencies of push−pull chromophores occurring in the visible region. The electronic polarization is the only contribution to the reaction field for nonpolar solvents, but in polar solvents a second contribution arises due to the reorientation of the polar solvent molecules around the solute. This orientational component of the reaction field has characteristic frequencies in the far-IR or microwave regions and is very slow with respect to both electronic and (internal) vibrational degrees of freedom of the solute.

The coupling of electrons to the fast solvent degrees of freedom can be dealt with in the antiadiabatic,[24] or sudden relaxation,[25] approximation. Since the fast degrees of freedom readjust instantaneously to the charge distribution of the solute molecule, the coupled problem can still be described in terms of a two-state model, but with renormalized parameters.[11] The amount of the renormalization can be evaluated given a microscopic model for the solute−solvent interaction.[11] However we adopt a different strategy, trying to extract all the relevant parameters from experimental data. For sure the parameters that describe the electronic structure of the solute (z_0 and $\sqrt{2}t$, or better their ratio) are expected to depend strongly on the solvent refractive index,[11] i.e., the square root of the dielectric constant as measured at optical frequencies, that offers a rough estimate of the electronic polarizability of the solvent. Then these "solute" parameters are actually transferable only among solvents with similar characteristics, specifically similar refractive index.

The orientational component of the reaction field at the equilibrium, F_{or}, is proportional to the solute dipole moment via a proportionality factor, r_{or}. Given a microscopic model for solute−solvent interaction, r_{or} can be easily estimated,[11] but, once more, we prefer extracting it from experiment. Eventually, the agreement between empirical and theoretical estimates will confirm the internal consistency of the proposed model. In the simplest picture, r_{or} depends on both the solvent refractive index and the (static) dielectric constant, vanishing for nonpolar solvents. By assimilating the solvent to an elastic medium, the following solvation term adds to the Hamiltonian in eq 1:[11]

$$H_{solv} = \frac{1}{2r_{or}} F_{or}^{\ 2} - F_{or}\hat{\mu} \qquad (2)$$

where the elastic constant is fixed by the equilibrium condition: $F_{or} = r_{or}\mu$ and μ represents the expectation value of $\hat{\mu}$. Basically, in this approximation the orientational component of the reaction field acts as an additional Holstein vibration. In fact, in the Mulliken approximation, the dipole moment operator is simply proportional to the ionicity operator, $\hat{\mu} = \mu_0\hat{\rho}$, and we can define an additional Holstein coordinate, Q_0, accounting for the solvent orientational degrees of freedom, whose characteristic relaxation energy is $\epsilon_{or} = r_{or}\mu_0^2/2$.[11] Of course the corresponding frequency and coupling constant are not well-defined, but, as we will see in the following, they do not explicitly enter any equation. The total Hamiltonian for a push−pull chromophore immersed in a solvent is then given by eq 1, provided the summation extends from 0 to N.[14]

In the adiabatic approximation,[26] an effective electronic Hamiltonian can be obtained from the total Hamiltonian in eq 1 by substituting the Q_i coordinates with the corresponding equilibrium values. The resulting two-state model has the same form as the original model, but with z_0 self-consistently depending on ρ, the expectation value of the ionicity operator.[10] The self-consistent DA dimer model can be solved exactly to get, e.g., the ground-state ionicity. Its dependence on z_0 is fairly interesting: the slope of the S-shaped $\rho(z_0)$ curve strongly increases with $\epsilon_T = \epsilon_{sp} + \epsilon_{or}$. Since the successive derivatives of the ρ vs z_0 curve are proportional to the static optical susceptibilities, one immediately recognizes a large amplification of static NLO responses as due to the coupling to slow degrees of freedom.[10,11]

In a two-state model a single parameter (either z_0 or ρ) defines not only the gs, but, in view of the orthogonality requirement, also the excited state. Specifically, the vertical excited state has ionicity $1 - \rho$, so that the vertical absorption energy and the corresponding transition dipole moment are

$$\omega_{CT} = \frac{1}{\sqrt{\rho(1-\rho)}} \qquad \mu_{CT} = \mu_0\sqrt{\rho(1-\rho)} \qquad (3)$$

In the harmonic approximation, the Huang−Rhys factors for the absorption process are simply proportional to the difference of ionicity in the two states, as follows: $S_i^{(abs)} = g_i(1 - 2\rho)/\omega_i$.[12] The dependence of ω_{CT}, μ_{CT} and of the absorption bandshape on the solvent stems out quite naturally from the dependence of ρ (the chromophore polarity) on the solvent.

The vertical excited state reached on photon absorption has in general a different polarity, and hence a different dipole moment, than the gs. Immediately after absorption, the slow degrees of freedom (internal vibrations and the solvent orientational modes) readjust themselves in response to the new charge configuration of the solute. But, as long as the slow degrees of freedom relax, the solute molecule itself feels a new surrounding and in turn readjusts its polarity. Whereas this picture holds true for all chromophores, the rearrangement of the solute polarity during the slow-mode relaxation is certainly large and nonnegligible for molecules with large NLO responses. The nonlinear, self-consistent relaxation problem can be solved exactly in our simple picture to calculate the equilibrium ionicity of the fully relaxed excited state, $1 - \rho^*$, as detailed in ref 12. The steady-state emission is once more a vertical process, that, starting from the relaxed excited state at ionicity $1 - \rho^*$, drives the system to the orthogonal gs, at ionicity ρ^*. The emission frequency and transition dipole moment, are still given by the same equations governing absorption, see eq 3, but with ρ^* substituting ρ. The Huang−Rhys factors for emission, $S_i^{(em)} = g_i(1 - 2\rho^*)/\omega_i$, are always smaller, in absolute value, than those relevant to absorption, then explaining the observation of narrower and less structured emission than absorption bands.[12,14] The same argument also naturally explains the narrowing of emission bands as observed for several chromophores in time-resolved emission measurements.[4,27]

Vibrational Spectra

It is fairly obvious that e−ph coupling largely affects vibrational properties of push−pull chromophores. In fact the vibrational properties of the DA dimer with Holstein coupling have already been investigated to model vibrational spectra of

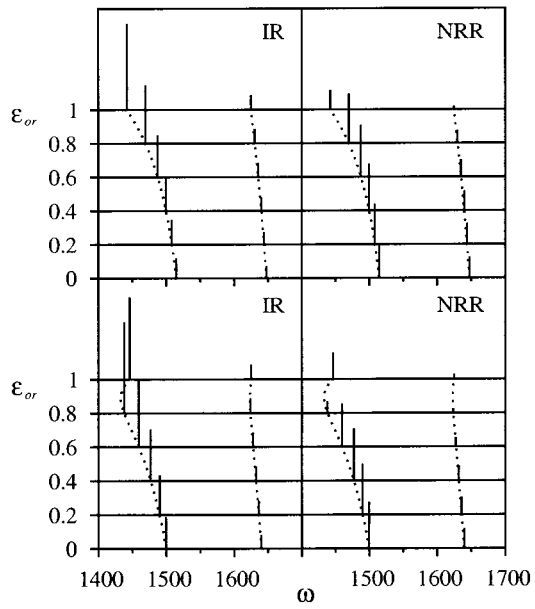

Figure 2. Equilibrium vibrational properties for a chromophore with two coupled internal vibrations: $\omega_1 = 0.19$, $g_1 = 0.15$, $\omega_2 = 0.21$, $g_1 = 0.29$; upper and lower panels refer to $z_0 = 0.8$ and 0.7, respectively. By choosing $\sqrt{2}t = 1$ eV, the x-axis is in cm^{-1}. Dotted lines show the dependence of equilibrium vibrational frequencies on solvent polarity (ϵ_{or}). For selected ϵ_{or} values, the vertical lines show the equilibrium IR and NRR intensities.

CT salts with a dimerized mixed stack motif.[28] Here we simply review the relevant results for push−pull chromophores.[10] The Hamiltonian in eq 1 defines the two harmonic surfaces relevant to $|DA\rangle$ and $|D^+A^-\rangle$ as having the same frequencies, but with finite coordinate displacements (see Figure 1). The mixing of the two states into the electronic ground and excited states will in general lead to a deformation of the originally harmonic surfaces. At the first order, the mixing only implies a shift of the two surfaces to the new equilibrium positions, the consequences of this shift on electronic spectra having been discussed in the previous section. At the second order, the mixing implies a variation of the harmonic frequencies relevant to the two states, and at higher orders anharmonic terms appear. Whereas anharmonic corrections can be important in push−pull molecules, here we discuss harmonic results, as a first guide to understand spectral properties.

The vibrational force constant matrix **F** can be calculated from the second derivatives of the gs energy with respect to the vibrational coordinates Q_i in eq 1:[21]

$$F_{ij} = \omega_i\omega_j\delta_{ij} - 2g_ig_j\sqrt{\omega_i\omega_j}\frac{\alpha_0}{{\mu_0}^2} \tag{4}$$

where δ_{ij} is the Kronecker-δ and $\alpha_0 = 2\mu_0{}^2[\rho(1-\rho)]^{3/2}$, is the electronic linear polarizability. The frequencies and normal modes of the coupled problem are obtained from the diagonalization of the force constant matrix. Overall, vibrational frequencies are softened by e−ph interactions. In the case of a single coupled mode, or for a mode well separated from other modes, the vibrational frequency is $\Omega_i = \omega_i\sqrt{1 - 2\epsilon_i\alpha_0/{\mu_0}^2}$.[11] More generally, e−ph coupling implies a mixing of vibrational coordinates, and the frequency of each mode depends on all coupling constants and frequencies.[21] In Figure 2, the dotted lines show the dependence of the frequencies of two coupled modes ($\omega_1 = 0.19$, $\omega_2 = 0.21$, $g_1 = 0.15$, $g_2 = 0.29$) on the solvent polarity. The upper panels refer to a fairly neutral chromophore ($z_0 = 0.8$), the bottom panels to a chromophore of intermediate ionicity ($z_0 = 0.7$). Force constant matrices of the same form as in eq 4 are typically obtained in models accounting for linear e−ph coupling. If $\alpha_0/\mu_0{}^2$ is assigned the role of a general electronic susceptibility, then eq 4 has already been written to describe vibrational properties of several classes of CT salts, of inorganic Pt−halogen chains, as well as of conjugated polymers.[22] In particular, curves similar to those presented in Figure 2 have already been drawn for polyacetylene (PA),[29] with the major difference that in that case the ordinate axis measures the electronic susceptibility, and in the present case the solvent polarity. Since the electronic susceptibility depends, via ρ, on the solvent polarity, the appearance of the two figures is similar. We underline that, just as it occurs in PA, by increasing the electronic susceptibility, the softening becomes more and more important for the lowest mode. The hardening of vibrational frequencies calculated for $z_0 = 0.7$ and $\epsilon_{or} > 0.9$ is easily understood in the same picture, since increasing the solvent polarity beyond $\epsilon_{or} \sim 0.9$ increases ρ beyond 0.5, and the electronic susceptibility starts decreasing.

The coupled internal vibrations are totally symmetric in the molecular point group, and are both IR and Raman active. Solvation effects are then expected in both spectra. Much as it occurs in other systems, e−ph coupling affects vibrational intensities.[22] In the case of a single (or isolated) mode, the IR and nonresonant Raman (NRR) intensities due to e−ph coupling, in the harmonic approximation, are given by[11]

$$I_{IR}^{(i)} = \left(\frac{\partial\mu_G}{\partial Q_i}\langle 0|Q_i|1\rangle\right)^2 = {g_i}^2\frac{{\alpha_0}^2}{{\mu_0}^2} \tag{5}$$

$$I_{NRR}^{(i)} = \left(\frac{\partial\alpha}{\partial Q_i}\langle 0|Q_i|1\rangle\right)^2 = {g_i}^2\frac{{\beta_0}^2}{{\mu_0}^2} \tag{6}$$

where $\beta_0 = 6\mu_0{}^3[\rho(1-\rho)]^2(1-2\rho)$ is the electronic contribution to the first hyperpolarizability. In the most general case of many coupled modes, the g_i's in the above equations have to be substituted by proper linear combinations in order to account for the mode mixing as inferred from the diagonalization of **F** in eq 4.[21] The mode mixing is responsible for a redistribution of vibrational intensities, as shown in the left and right panels of Figure 2 for the IR and NRR cases, respectively. Once more, just as it occurs in other systems characterized by large e−ph coupling, by increasing the electronic susceptibility, low-frequency modes borrow intensity from higher modes.[29]

Polar Solvents: A Model for Inhomogeneous Broadening

In the previous sections we have described the spectral properties of a solvated push−pull chromophore at the equilibrium, i.e., with both internal and solvation coordinates in the configuration that minimizes the total (solute+solvent) energy. At finite temperature (T), however, deviations from equilibrium are possible. In particular, the orientational modes of polar solvents, that are characterized by very low frequencies, are expected to be easily excited at room T. The simplest picture for thermal fluctuations in polar solvents considers the orientational component of the reaction field as slowly oscillating around its equilibrium value. Since this oscillation is much slower than all other degrees of freedom, including internal vibrations of the chromophore,[30] the solution can be modeled in terms of a Boltzmann distribution of chromophores each one in equilibrium with the local solvent configuration. The Boltzmann distribution explicitly introduces the T variable in the

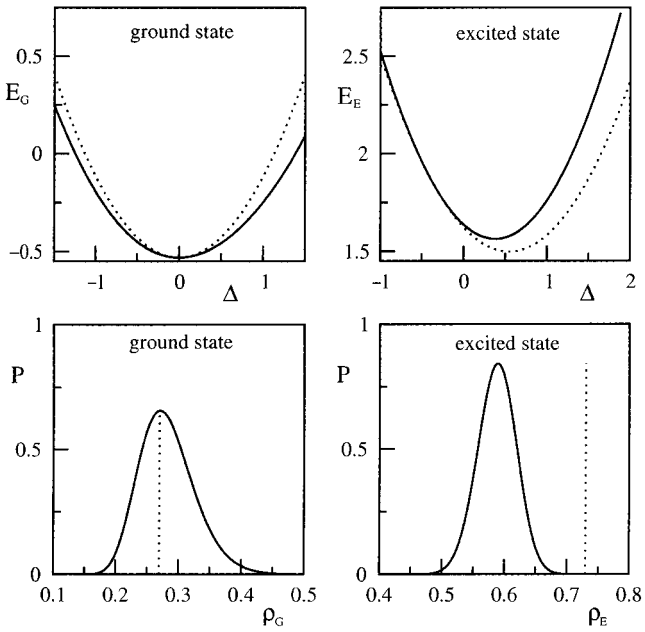

Figure 3. Upper panels: the solute + solvent energy vs the fluctuation of the orientational component of the reaction field (Δ), measured as deviation from the value relevant to the equilibrium gs for a chromophore with $z_0 = 0.8$, $\epsilon_{sp} = 0.45$ and for $\epsilon_{or} = 0.6$. Lower panels: probability distribution of the solute polarity, for the same parameters as before, and for $T = 300$ K. Left and right panels refer to the ground and excited state, respectively. Continuous and dotted lines refer to the exact model (polarizable solute picture) and to the perturbative treatment (rigid solute picture), respectively.

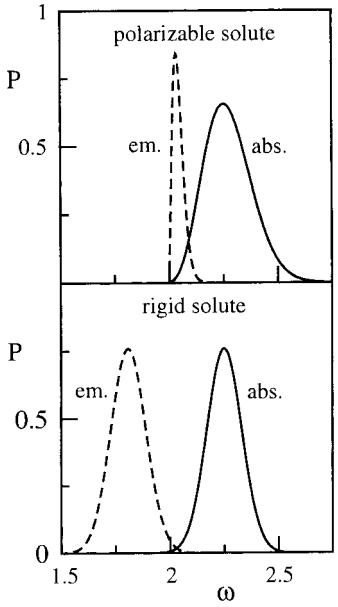

Figure 4. Probability distribution of transition energies (same parameters as in Figure 3), in arbitrary units, but with normalized areas. Continuous and dashed lines refer to absorption and steady-state emission processes, respectively. Upper panel: the exact model. Lower panel: the rigid solute picture.

equations. However it is important to recognize that ϵ_{or} is intrinsically a T-dependent quantity. In the simplest approaches,[3,13] the T dependence of ϵ_{or} is hidden in the T dependence of the solvent dielectric constant and/or refractive index. In more refined treatments,[30] the T dependence of the solvent polarization stems out more clearly. In any case, the T inserted in the Boltzmann distribution must coincide with the T implied by the choice of ϵ_{or}.

To account for the fluctuations of the orientational component of the reaction field around its equilibrium value (F_{or}), we simply substitute F_{or} in eq 1 with $F_{or} + \Delta$, Δ measuring the fluctuating field. The energy of the solute+solvent system and the solute properties can be easily calculated as a function of Δ. The Δ contribution to the solvent elastic energy is in fact trivial, and its contribution to the solute−solvent interaction (from the last term in eq 1) simply adds to z_0 the constant $-\Delta\mu_0/2$. Since the exact solutions of the Hamiltonian in eq 1 as a function of z_0 are known,[10] we immediately get the effects of Δ. In Figure 3, left upper panel, we report, as a function of Δ, the total energy of a solvated chromophore in its gs configuration (E_G) for the parameters $z_0 = 0.8$, $\epsilon_{sp} = 0.45$ and $\epsilon_{or} = 0.6$. The exact result (continuous line) accounts for the variation of solute polarity with Δ. In perturbative approaches to solute−solvent interaction, instead, the solute polarizability is neglected and ρ is kept fixed to its equilibrium value. Then the $E_G(\Delta)$ curve is a parabola with curvature $1/r_{or} = \mu_0^2/2\epsilon_{or}$. In Figure 3 the deviation of the exact curve from the parabolic behavior (dotted line) is apparent. More impressive is however the comparison between the probability distributions described by the two models. In the lower left panel in Figure 3 we report the distributions of the solute polarity: in the rigid model the probability distribution is a Dirac-δ (dotted line) centered at the equilibrium ρ. The exact result (continuous line), reported in the same figure for $T = 300$ K, shows instead a fairly large and slightly asymmetric ρ-distribution. Since, as discussed in the previous sections, the spectral properties of push−pull chromophores strongly depend on ρ, this broad distribution is the key to understand inhomogeneous broadening effects on spectral properties of push−pull chromophores in polar solvents.

Inhomogeneous broadening in electronic spectra can be accounted for in the rigid solute picture too. In this perturbative approach, in fact, the electronic energies are corrected up to the first order in the solute−solvent interaction,[13] so that they linearly depend on Δ, according to $-\Delta\mu$, μ representing the expectation value of the dipole moment operator in the relevant state. Figure 4 compares the exact probability distribution of absorption frequencies (continuous line, upper panel) with that obtained in the rigid solute approximation (continuous line, lower panel). The two distributions are fairly similar, the major difference being the slight asymmetry of the exact curve. Since absorption band-shapes are obtained by convoluting the distribution with the relevant vibronic structure, the two distributions can be considered essentially equivalent for all practical purposes.

Something qualitatively different occurs for emission. In Figure 3, right upper panel, we compare the exact Δ dependence of the energy of the steady-excited state (continuous line) with the rigid solute result (dotted line). The fluctuations of the solvent orientational field (Δ) are measured as deviations from the field in equilibrium with the gs, so that both the exact and approximate curves have minima at $\Delta \neq 0$. In the rigid solute picture, the Δ dependence of the excited state energy is exactly the same as for the gs. Deviations from the parabolic behavior are apparent for the exact curve, but what is more important is that the exact and approximate curves have minima at different positions. This is of course related to the different polarity (i.e., to the different dipole moments) characterizing the steady-excited state in the two approaches. The difference is even more apparent in the lower right panel, showing the corresponding ρ-distributions. In the rigid solute picture, the distribution is a Dirac-δ (dotted line) centered at $1 - \rho$, ρ measuring, as usual, the gs polarity. The exact picture predicts a broad distribution (continuous line), centered at a different ionicity, $1 - \rho^*$, as

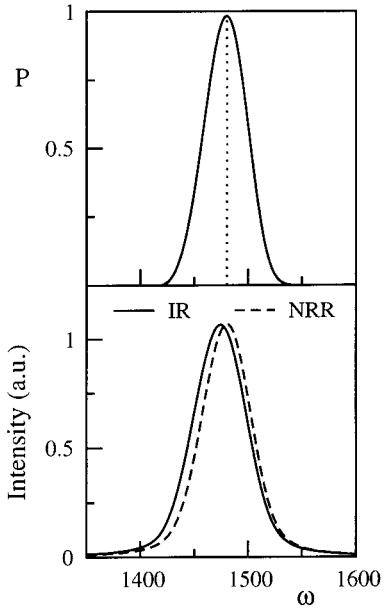

Figure 5. Upper panel: probability distribution of the vibrational frequency of a single coupled mode having $\omega_v = 0.2$, for the same parameters as in Figure 3. Lower panel: IR and NRR spectra calculated for the intrinsic line width of vibrational states, $\gamma = 8$ cm^{-1}. X-axis in cm^{-1}.

discussed in the previous section. This has fairly obvious consequences on emission frequencies, that in the rigid solute picture are always underestimated (see Figure 4). More subtle is the effect on band-shapes: since absorption (or equivalently emission) frequencies nonlinearly depend on the polarity of the involved states, the exact distribution of emission frequencies (Figure 4, upper panel, dashed line) turns out always narrower than that obtained in the rigid solute picture (Figure 4, lower panel, dashed line).

The rigid solute picture accounts for inhomogeneous broadening in electronic absorption or emission bands, but it cannot reproduce *both* spectra in terms of the *same* microscopic parameters. On the other hand, the rigid solute picture cannot account for solvation effects in vibrational spectra. In fact, vibrational excitations do not modify the molecular dipole moment, so that in the rigid solute approximation there are no corrections to vibrational energies due to solvation. In the previous section we demonstrated that, since the equilibrium polarity (ρ) of the polarizable solute depends on the solvent, then vibrational frequencies depend on the solvent too (see Figure 2). Similarly, since the fluctuations of the orientational component of the reaction field around the equilibrium affect the solute polarity, our model naturally predicts inhomogeneous broadening of vibrational spectra of push−pull chromophores dispersed in polar solvents. On the basis of the same gs distribution as reported in Figure 3, left lower panel, and on the ρ dependence of the frequencies of the coupled modes, as implied by eq 4, we calculate the probability distribution of the vibrational frequency, Ω_v, of a single coupled mode, as reported in Figure 5, upper panel. The Ω_v-distribution is the key to understand vibrational inhomogeneous broadening, but due to the nonlinear dependence of IR and/or NRR intensities on ρ (see eqs 5 and 6), it does not offer direct spectral information. By weighting the distribution in Figure 5 with the IR and NRR intensities in eqs 5 and 6, we calculate the corresponding spectra as reported in Figure 5, lower panel, where the homogeneous bands are modeled as single Lorentzians with half-width at half-maximum $\gamma = 8$ cm^{-1}. The inhomogeneous broadening as due to the solvent polarity is very well apparent. More interesting,

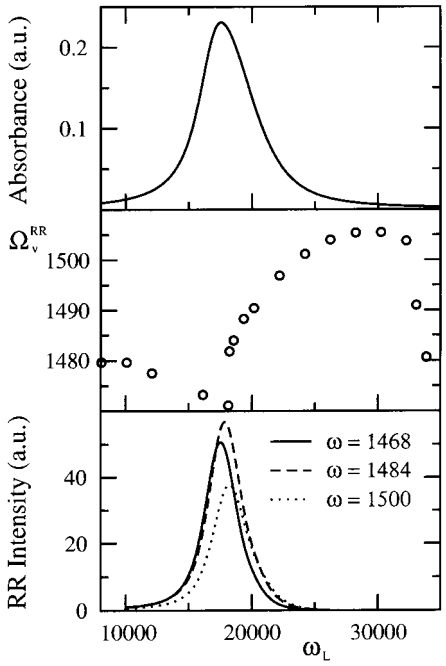

Figure 6. Absorption and RR spectra for a chromophore with the same parameters as in Figure 5 and intrinsic electronic line width $\Gamma = 1600$ cm^{-1}. Upper panel: absorption spectra. Middle panel: dependence of the RR frequency on the excitation line. Lower panel: RR excitation profiles calculated for the selected vibrational frequencies displayed in the legend. Frequencies in cm^{-1}.

however, is the observation of different frequencies in IR and NNR spectra. This is of course due to the markedly different ρ-depedendence of I_{IR} and I_{NRR}, particularly at $\rho \sim 0.5$. As it turns out from the figure, the large inhomogeneous broadening suffered by coupled modes implies that, for push−pull chromophores dispersed in polar solvents, the same vibrational mode can appear with different frequencies in IR and NRR spectra. The experimental determination of the corresponding frequencies shifts is not easy, but is interesting to pursue.

Inhomogeneous broadening affects both electronic and vibrational states, and therefore its most impressive effects are expected in RR spectra. Figure 6 shows some results obtained for the model parameters discussed above. The upper panel reports the absorption spectrum calculated in the Condon approximation. According to the previous discussion, inhomogeneous broadening is taken into account by summing over the Condon spectra calculated for each ρ, weighted by the ρ-distribution in Figure 3. Each vibronic line is modeled as a Lorentzian with half-width at half-maximum, $\Gamma = 1600$ cm^{-1}. Analogously, inhomogeneously broadened RR spectra can be calculated as sum over the ρ distribution of the homogeneous RR spectra relevant to each ρ. Specifically, for each ρ the homogeneous RR spectrum is defined by a single Lorentzian centered at the relevant frequency Ω, with intrinsic vibrational line width, γ, and whose intensity is given by the square of the Raman polarizabilty, α_R. In the harmonic approximation, the standard vibronic expansion of the transition dipole moments,[31] gives the following equation for α_R:

$$\alpha_R = \sum_v \left(\mu_{CT}\langle 0|v\rangle + \frac{\partial \mu_{CT}}{\partial Q}\langle 0|Q|v\rangle\right)\left(\mu_{CT}\langle v|0\rangle + \frac{\partial \mu_{CT}}{\partial Q}\langle v|Q|0\rangle\right) \times \left(\frac{1}{\omega_{Ev} + \omega_R + i\Gamma} + \frac{1}{\omega_{Ev} - \omega_L + i\Gamma}\right) \quad (7)$$

where ω_L and ω_R are the Laser and Raman frequencies, respectively, $|0\rangle$ and $|1\rangle$ are the zero- and one−phonon states of the ground electronic state, $|v\rangle$ is the vibrational state of the excited manifold with v phonons, ω_{Ev} is the frequency of the transition from the ground vibronic state to the excited state with v phonons, and Γ is the corresponding line width, that is set equal to the electronic homogeneous line width. The transition dipole moment is easily calculated, within the Herzberg−Teller approach,[10,11] as $\partial\mu_{CT}/\partial Q = \sqrt{2\omega}g(1 - 2\rho)\mu_{CT}/\omega_{CT}$. The above equation can be easily extended to the multimode case.

The effects of inhomogeneous broadening in RR spectra are impressive: by tuning ω_L within the absorption band, molecules with matching absorption frequencies are preferentially excited. So, at different ω_L, one observes RR scattering from molecules with different ρ, and then with different vibrational frequencies. Depending on the model parameters, chromophores dispersed in polar solvents can show a large dispersion of RR frequencies with the excitation line. Although with different physical origins, the mechanism responsible for the RR dispersion in push−pull chromophores in solution is exactly the same as acting in PA:[32,33] in PA samples, segments of different conjugation length are characterized by different absorption and vibrational frequencies; in solvated push−pull chromophores a distribution of molecules with different electronic and vibrational frequencies is originated by thermal disorder in the solvation cage. Figure 6, middle panel, shows the dependence of the position (first moment) of the RR band, Ω_v^{RR}, as a function of ω_L as calculated for the same parameters as before. For ω_L well below (or above) the absorption band we indeed measure a NRR spectrum, and $\Omega_v^{RR} \rightarrow \Omega_v^{NRR}$ (cf. Figure 5). The minimum frequency is obtained by exciting slightly below the absorption maximum, where molecules with $\rho \sim 0.5$ are preferentially excited. By increasing further ω_L, molecules with ρ deviating from 0.5 are excited, and Ω_v^{RR} increases. Similar information can be gained from the excitation profiles (lowest panel in Figure 6). At vibrational frequencies lower than the equilibrium vibrational frequency, the RR intensity maximizes at fairly low frequencies (lower than the absorption maximum); at higher vibrational frequencies, the maximum RR intensity moves higher in energy.

Conclusions

In this paper, the self-consistent DA dimer model, previously proposed to describe push−pull chromophores, is solved to get a nonperturbative description of optical (electronic and vibrational) spectra of these molecules in solution. Previous work on electronic (absorption and emission) spectra[12] is extended here to explicitly include inhomogeneous broadening as due to the coupling to slow (orientational) degrees of freedom of polar solvents. The extensive discussion of vibrational properties of push−pull chromophores in solution points to several interesting features. First of all we predict a large dependence of vibrational (IR and Raman) frequencies and intensities on the solvent polarity, with softening and mode mixing phenomena that share several common features with other systems characterized by large linear e−ph coupling[22] (CT salts, conjugated polymers, inorganic Pt−halogen chains). Even more interesting are inhomogeneous broadening effects. Apart from the broadening of observed vibrational bands with increasing solvent polarity, we predict, for molecules where broadening is most effective, the noncoincidence of IR and NRR frequencies, and the dispersion of RR frequencies with the excitation line. In the companion paper we will apply the present model to discuss spectral properties of an interesting chromophore, phenol blue (PB). The exotic spectral behavior of PB is fairly naturally understood based on our simple model. Specifically, fixed a few model parameters, PB electronic absorption spectra, as well as IR, NRR and RR spectra measured in different solvents are well reproduced. The good agreement with experiment proves the validity of the model and the possibility to extract a reliable set of microscopic parameters from the combined analysis of spectral data.

Experimental studies of the solvent dependence of electronic *and* vibrational spectra of push−pull chromophores are still scanty, PB representing an interesting and fortunate exception. More extensive experimental data are required for a wider test of the proposed model. We hope that some interest in this field will be triggered by the present study, that points to new and interesting spectral features of solvated push−pull chromophores and shows that a more sound understanding of the properties of these interesting molecules can be obtained from an extensive spectral analysis.

The two-state model we adopt to describe the electronic structure of push−pull chromophores is certainly an oversimplified model. Whereas the comparison with experimental data proves it works well for a few chromophores, we do not really believe it applies to all chromophores. Just as an example, chromophores with fairly long polyenic spacers are expected[34] (and are indeed observed[35]) not to be modeled adequately in terms of two states. Quite irrespective of its accuracy and/or applicability, our simple model, with its exact solutions, teaches us a few important lessons of general validity, the most important one being the inadequacy of linear perturbative treatments of interactions in systems with highly nonlinear behavior. In these systems, and therefore in all systems with large NLO susceptibilities, improving simple models to include higher states and/or making resort to extensive quantum chemical calculations is totally useless if the relevant interactions (e.g., e−ph and solute−solvent interactions) are perturbatively dealt with. The far-reaching implications of the system nonlinearity on the calculation of NLO responses[10,11] and on the interpretation of solvatochromic shifts have already been discussed.[12] Here we want to underline a general and important consequence of nonlinearity on spectral properties: highly nonlinear molecules are highly polarizable, so that the electronic states largely respond to the configuration of slow variables. The states involved in vertical processes taking place at different points in the configuration space of slow variable (e.g., absorption and steady-state emission) are different. For the same reasons the electronic states involved in vertical processes (e.g., emission) and horizontal processes (e.g., electron transfer) are different. For nonlinear systems, like push−pull chromophores, the spectral parameters, like Huang−Rhys factors, obtained from the analysis of a vertical process are not relevant to a different vertical process, nor are they directly transferable to describe electron transfer process. Extracting microscopic information from optical spectra is, for materials with nonlinear behavior, a highly nontrivial process, and many of our current approaches need to be critically reconsidered.

Acknowledgment. We thank A. Girlando for useful discussions. Work was supported by the Italian National Research Council (CNR) within its "Progetto Finalizzato Materiali Speciali per Tecnologie Avanzate II", and by the Ministry of University and of Scientific and Technological Research (MURST).

References and Notes

(1) Kanis, D. R.; Ratner, M. A.; Marks, T. J. *Chem. Rev.* **1994**, *94*, 195.
(2) Marder, S. R.; Kippelen, B.; Jen, A. K−Y.; Peyghambarian, N. *Nature* **1997**, *388*, 845.
(3) Reichardt, C. *Chem. Rev.* **1994**, *94*, 2319.
(4) Horng, M. L.; Gardecki, J. A.; Papazyan, A.; Maroncelli, M. *J. Phys. Chem.* **1995**, *99*, 17311.
(5) Myers Kelley, A. B. *J. Phys. Chem. A* **1999**, *103*, 6891.
(6) Oudar, J. L.; Chemla, D. S. *J. Chem. Phys.* **1977**, *66*, 2664.
(7) Mulliken, R. S. *J. Am. Chem. Soc.* **1952**, *74*, 811.
(8) Wynne, K.; Galli, C.; Hochstrasser, R. M. *J. Chem. Phys.* **1994**, *100*, 4797.
(9) Soos, Z. G.; Keller, H. J.; Moroni, W.; Nöthe, D. *Ann. N. Y. Acad. Sci.* **1978**, *313*, 442.
(10) Painelli, A. *Chem. Phys. Lett.* **1998**, *285*, 352.
(11) Painelli, A. *Chem. Phys.* **1999**, *245*, 183. Painelli, A. *Chem. Phys.* **2000**, *253*, 393.
(12) Painelli, A.; Terenziani, F. *Chem. Phys. Lett.* **1999**, *312*, 211.
(13) Liptay, W. *Angew. Chem.* **1969**, *8*, 177; In *Excited States*; Lim, E. C., Ed.; Academic: New York, 1974; p 129.
(14) Painelli, A.; Terenziani, F. *Synth. Met.* **2000**, *109*, 229.
(15) Yamaguchi, T.; Kimura, Y.; Hirota, N. *J. Phys. Chem. A* **1997**, *101*, 9050.
(16) Yamaguchi, T.; Kimura, Y.; Hirota, N. *J. Chem. Phys.* **1998**, *109*, 9075. Yamaguchi, T.; Kimura, Y.; Hirota, N. *J. Chem. Phys* **1997**, *107*, 4436.
(17) Markel, F.; Ferris, N. S.; Gould, I. R.; Meyers, A. B. *J. Am. Chem. Soc.* **1992**, *114*, 6208.
(18) Myers, A. B. *Chem. Phys.* **1994**, *180*, 215.
(19) Marder, S. R.; Beratan, D. N.; Cheng, L.-T. *Science* **1991**, *252*, 103.
(20) See, e.g.: Schatz, G. C.; Ratner, M. A *Quantum Mechanics in Chemistry*; Prentice Hall International: Englewood Cliffs, NJ, 1993.
(21) Painelli, A.; Girlando, A. *J. Chem. Phys.* **1986**, *84*, 5665.
(22) Girlando, A.; Painelli, A.; Soos, Z. G. *Acta Phys. Pol. A* **1995**, *87*, 735.
(23) Di Bella, S.; Marks, T. J.; Ratner, M. A. *J. Am. Chem. Soc.* **1994**, *116*, 4440.
(24) Feinberg, D.; Ciuchi, S.; De Pasquale, F. *Int. J. Mod. Phys.* **1990**, *4*, 1317.
(25) Fortunelli, A.; Painelli, A. *Chem. Phys. Lett.* **1993**, *214*, 402.
(26) Longuet-Higgins, H. C. *Adv. Spectrosc.* **1961**, *2*, 429.
(27) Fee, R. S.; Maroncelli, M. *Chem. Phys.* **1994**, *183*, 235.
(28) Girlando, A.; Bozio, R.; Pecile, C.; Torrance, J. B. *Phys. Rev. B* **1982**, *26*, 2306.
(29) Girlando, A.; Painelli, A.; Soos, Z. G. *Chem. Phys. Lett.* **1992**, *198*, 9.
(30) Loring, R. F.; Yan, Y. J.; Mukamel, S. *J. Chem. Phys.* **1987**, *87*, 5840. Loring, R. F.; Yan, Y. J.; Mukamel, S. *Chem. Phys. Lett.* **1987**, *135*, 23.
(31) Tang, J.; Albrecht, A. C. *Raman Spectroscopy*; Plenum: New York, 1970; Vol. 2.
(32) Cataliotti, R. S.; Paliani, G.; Dellepiane, G.; Fuso, S.; Destri, S.; Piseri, L.; Tubino, R. *J. Chem. Phys.* **1985**, *82*, 2223.
(33) Masetti, G.; Campani, E.; Gorini, G.; Piseri, L.; Tubino, R.; Dellepiane, G. *Sol. State Comm.* **1985**, *55*, 737.
(34) Tretiak, S.; Chernyak, V.; Mukamel, S. *Chem. Phys.* **1999**, *245*, 145.
(35) Castiglioni, C. Private communication.